




## Research Article

# A Tuned Mass Damper with Nonlinear Magnetic Force for Vibration Suppression with Wide Frequency Range of Offshore Platform under Earthquake Loads

Qiong Wu <sup>1,2</sup>, Wei Zhao,<sup>3</sup> Weiguo Zhu,<sup>1</sup> Rencheng Zheng <sup>1,4</sup> and Xilu Zhao <sup>2</sup>

<sup>1</sup>Jiangsu Key Laboratory of Advanced Manufacturing Technology, Huaian 223003, China

<sup>2</sup>College of Mechanical Engineering, Saitama Institute of Technology, Saitama 3690293, Japan

<sup>3</sup>Global Axis Inc., Mida Minato, Tokyo 1080073, Japan

<sup>4</sup>School of Automotive Engineering, Dalian University of Technology, Dalian 116024, China

Correspondence should be addressed to Rencheng Zheng; topzrc@dlut.edu.cn

Received 13 March 2018; Revised 4 July 2018; Accepted 18 July 2018; Published 16 August 2018

Academic Editor: Evgeny Petrov

Copyright © 2018 Qiong Wu et al. This is an open access article distributed under the Creative Commons Attribution License, which permits unrestricted use, distribution, and reproduction in any medium, provided the original work is properly cited.

Tuned mass dampers (TMDs) are applied to ensure the safety and stability of offshore platforms; however, linear dampers are effective for a single resonance frequency, providing vibration suppression only within a narrow frequency band. Therefore, this paper proposed a magnetic TMD with two pairs of permanent magnets on both sides of the structures, which can generate a nonlinearly repulsive force, making the magnetic TMD reliable and robust in damping the oscillations of structures with wide frequency range under seismic excitations. A comprehensively numerical and experimental study was processed to investigate the dynamic performances of the proposed magnetic TMD, by application of a 1:200-scale prototype of the offshore platform. The results verified that the performance of the magnetic TMD can be significantly improved than that of the linear TMD, meanwhile maintaining high-speed response characteristics. The experimental results indicated that the displacement, acceleration, and frequency responses of the offshore platform can be significantly reduced; furthermore, the evaluation indices showed that the magnetic TMD system is credible in reducing the overall vibration levels and maximum peak values.

## 1. Introduction

An offshore platform located in ocean environments is unavoidably affected by external disturbance, such as winds, water waves, and earthquakes. The large vibration amplitude can damage the structures or the secondary components and cause discomfort to its human occupants [1]. Extensive research had been conducted to mitigate this harmful vibration, for example, structure design [2], vibration isolation systems, and auxiliary damping systems [3]. Among these methods, the tuned mass damper (TMD) has been proved to be a simple and effective vibration suppression device. Although a linear TMD is effective in attenuating vibration at a specific excitation frequency, perhaps the most significant

limitation is its narrow effective bandwidth in the frequency domain. When the natural frequency of the primary structure shifts due to structural degradation or other reasons, a linear TMD can act instead as a vibration amplifier, increasing the response amplitude of the primary structure. This problem has received considerable attention from researchers in the past.

In an attempt to overcome this limitation, initially, such a drawback can be overcome through use of multiple tuned mass dampers, of which each TMD is tuned to a specific frequency of the main system [4–6]. The wideband multiple TMD system has been developed for reducing the multiple resonant responses of the main structure. However, because the TMD mass has to be divided into many smaller ones,

practical applications of multiple TMD approach still have some limitations, and the other problem is too big to introduce here. Some other efforts construct multi-DOF single mass TMD [7, 8].

In the last decades, to overcome the drawbacks of passive TMDs due to detuning, the researchers investigated an undamped nonlinear dynamic vibration absorber system. Kwag et al. [9] proposed and developed the concept of an eddy current shock absorber using permanent magnets; moreover, the absorber was constructed, and the experiments were performed to investigate its dynamic characteristics. Cai et al. [10] studied on a conceptual exploration of the magnetorheological TMD system for cable vibration mitigation through an experimental approach. The developed damper can absorb the cable vibration energy through both the TMD component and the magnetorheological component. Afterwards, Ayala-Garcia et al. [11] presented a new magnetic tuning mechanism which can be operated by modifying the effective spring constant of the system in the mechanical domain. Eason et al. [12] used a standard tuning approach for the nonlinear TMD and comparing its performance with an optimal passive linear TMD. Viet and Nghi [13] explained the nonlinearity of the pendulum to increase the number of DOF of the TMD, and it had better performance at large vibration and was less sensitive than the linear TMD. Gourdon et al. [14] experimentally confirmed that nonlinear TMD can irreversibly extract some of the energy from the structure to which they are attached. Additional studies [15–18] had demonstrated that a nonlinear TMD requires a much smaller mass than a linear TMD to achieve identical reduction effects and is capable of attenuating the transient oscillations of a main structure more effectively, and the nonlinearity can be added by the cubic spring or by the impact.

On the other hand, for more than two decades, the application of magnetic eddy currents for damping purposes has been investigated. Sodano et al. [19] have analyzed the suppression of cantilever beam vibrations, where a permanent magnet is fixed so that it is perpendicular to the beam motion, and a conducting sheet is attached to the beam tip. Then, a theoretical model of an eddy current damper was modified and further developed by applying an image method to satisfy the boundary condition of the zero eddy current density at the conducting plate boundaries [20]. Kwak et al. [21] developed a damping concept to suppress the vibration of a cantilever beam using eddy currents. This system consists of a copper plate mounted to the free end of the beam and a flexible linkage with two magnets. Later, Bae et al. [22] developed a mathematical model of this system and simulated the response using a numerical solution. Both the model and experiments showed the effectiveness of this damping mechanism. Zhang and Ou [23] performed theoretical and experimental studies on the active vibration control of two-story shear building using an electromagnetic mass damper. Kim et al. [24] investigated active vibration control of the vehicle suspension system using an electromagnetic damper. Palomera-Arias et al. [25] utilized an electromagnetic device as a passive damper and studied the modeling of electromagnetic damping coefficient and the

feasibility of using it for building vibration control. Wu et al. [26, 27] proposed the passive damper of an offshore platform against stroke energy and response delay problems under seismic waves. Both simulation and experimentation studies were proposed to verify the effectiveness and advantages of the proposed methods.

However, though application of the magnetic spring effect in vibration suppression has been reported, to the best of the authors' knowledge, application of a TMD damper with a magnetic spring effect has not been examined in the previous publications, especially for vibration suppression of offshore platform under earthquake loads. Therefore, this paper tried to present a new magnetic tuning mechanism which can operate by modifying the effective spring constant of the system in the mechanical domain, and a pair of permanent magnets is applied to create a repulsive force that is proportional to the velocity of the conductor, and the moving magnet and conductor behave as a variable-stiffness spring. In this way, the nonlinear magnetic force can be utilized for a number of different applications.

In this study, the effectiveness of the nonlinear TMD for vibration control of a seismically excited offshore platform structure is evaluated, and an experimental model of the offshore platform with the nonlinear TMD is developed. The nonlinear TMD device has a single-mass block with two pairs of permanent magnets, and the repulsive force between the permanent magnets is produced by a variable-stiffness spring, providing the damper with a wide operational frequency range. The magnet damper is a noncontact type passive damper, it transfers energy from the main structure by the relative motion, and the control structure interaction is just the offset forces between the substructure and main structure; it has the effectiveness to vibration reduction. Moreover, this paper involves experimental and analytical investigations that comprehensively extend the understanding of the wide frequency range performance and damping characteristics of a magnetic nonlinear TMD system under three strong seismic vibrations.

## 2. Methods and Materials

*2.1. Modeling.* To analyze the effectiveness of the TMD, an actual jackup offshore platform, Bohai no. 5 located in the Southern Sea, was considered as the research target. As shown in the left panel of Figure 1, the jackup offshore platform comprises a rectangular platform resting on four independent operating legs, with a TMD attached beneath the platform. The size of the working platform is  $57.5 \times 34.0 \times 5.50$  m, the length and diameter of the operating legs are 78 and 3 m, respectively, and the limit of the operating water depth is 40 m. As shown in the right panel of Figure 1, an experimental model was constructed based on a 1:200-scale model of an actual four-column jackup offshore platform.

*2.2. Nonlinear Magnetic Elastic Coefficient Measurement.* A prototype experiment model was built in the laboratory as shown in Figure 2(a). The TMD device consists of a frame,

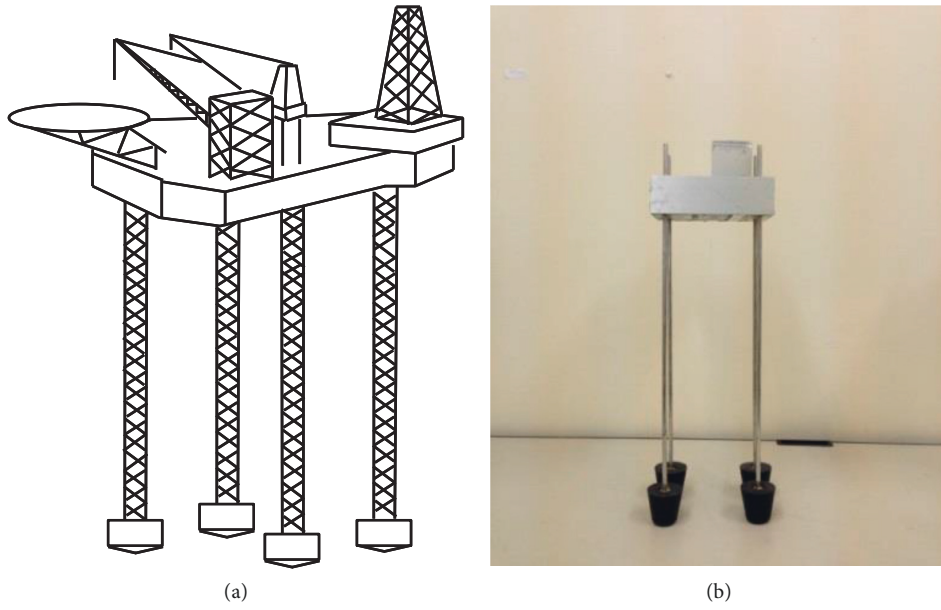


FIGURE 1: Jackup offshore platform (a) and 1 : 200-scale model (b).

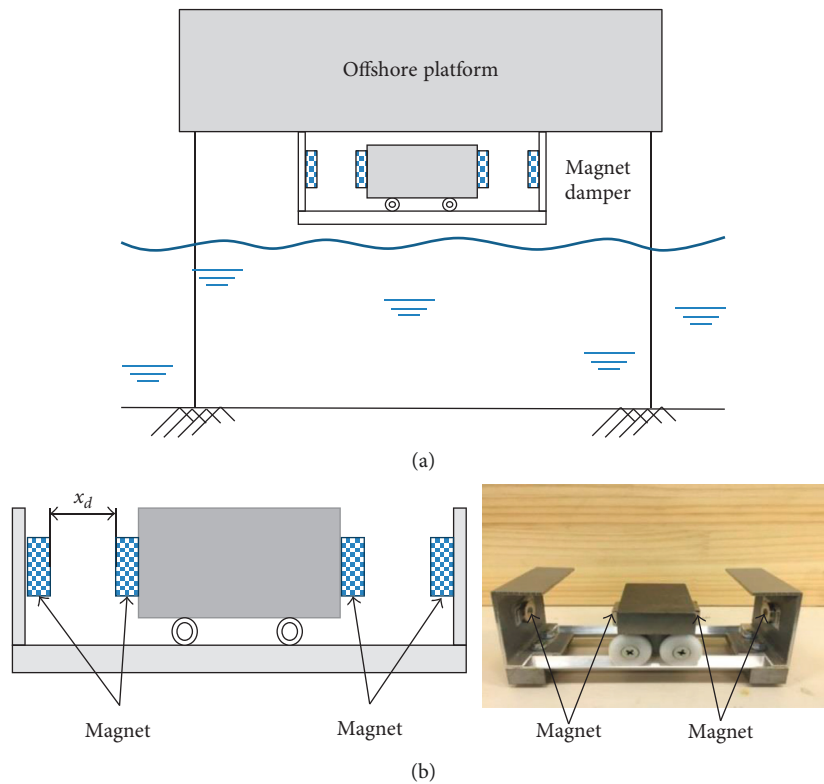


FIGURE 2: Experimental model of the magnet TMD. (a) Jackup offshore platform with a magnet TMD; (b) model of magnet TMD.

a mass, two springs, four wheels, two tracks, and two pairs of permanent magnets, as shown in Figure 2(b).  $x_d$  is the gap between the pair of permanent magnets as shown in Figure 2(b). When the TMD is working, the permanent magnets generate a time-varying magnetic force which is inversely proportional to the gap  $x_d$ . The variable magnetic forces act like a variable-stiffness spring. Thus, when the

offshore platform's natural frequency changes, the magnet TMD can dampen the vibration by slightly adjusting the natural frequency of the magnet TMD system and match it with the targeted resonant excitation frequency. Here, the material of the TMD's mass block is steel, and it will have a bad influence with the magnetic field. For avoiding this effect, the TMD was well tinned.

Before carrying out the vibration experiment, the basic characteristics of the magnetic force were obtained. Figure 3 shows the calculation diagram of the permanent magnet repulsive force. About geometry of the two permanent magnets as shown in Figure 3(a),  $l$ ,  $w$ , and  $h$  are the length, width, and height of the magnet, respectively.  $d$  is distance of the two permanent magnets.  $F_m$  is the repulsive force. The repulsive force of the two permanent magnets can be expressed as follows [28]:

$$F_m = \frac{1.5}{1 + 3d} \times \frac{1}{2u_0} B^2 wh, \quad (1)$$

where  $B$  is the flux density and  $u_0$  is the permeability of space. The flux density of the permanent magnets can be expressed as

$$B = \frac{B_r}{\pi} \left( \tan^{-1} \frac{wh}{2d\sqrt{w^2 + h^2 + 4d^2}} - \tan^{-1} \frac{wh}{2(l+d)\sqrt{w^2 + h^2 + 4(l+d)^2}} \right), \quad (2)$$

where  $B_r$  is the magnetic property of permanent magnets. Equation (1) can be substituted into (2) to calculate the repulsive force of the two permanent magnets as

$$F_m = \frac{1.5}{1 + 3d} \times \frac{wh}{2u_0} \times \left[ \frac{B_r}{\pi} \left( \tan^{-1} \frac{wh}{2d\sqrt{w^2 + h^2 + 4d^2}} - \tan^{-1} \frac{wh}{2(l+d)\sqrt{w^2 + h^2 + 4(l+d)^2}} \right) \right]^2. \quad (3)$$

As shown in Figure 3(b), the resultant repulsive force  $F_r$  of the magnetic field is concerned at both ends of the mass block of the tuned mass damper, which can be expressed as

$$\begin{aligned} F_r &= F_{m1} - F_{m2} \\ &= \frac{1.5}{1 + 3d_1} \times \frac{wh}{2u_0} \times \left[ \frac{B_r}{\pi} \left( \tan^{-1} \frac{wh}{2d_1\sqrt{w^2 + h^2 + 4d_1^2}} - \tan^{-1} \frac{wh}{2(l+d_1)\sqrt{w^2 + h^2 + 4(l+d_1)^2}} \right) \right]^2 \\ &\quad - \frac{1.5}{1 + 3d_2} \times \frac{wh}{2u_0} \\ &\quad \times \left[ \frac{B_r}{\pi} \left( \tan^{-1} \frac{wh}{2d_2\sqrt{w^2 + h^2 + 4d_2^2}} - \tan^{-1} \frac{wh}{2(l+d_2)\sqrt{w^2 + h^2 + 4(l+d_2)^2}} \right) \right]^2. \end{aligned} \quad (4)$$

In this experiment, the material parameters of magnet are shown in Table 1.

As shown in Figure 4, the measurement setup was prepared in order to verify the correctness of the mathematical model. It consisted of a force measuring device, a fixed fixture, and a ruler. The force measuring device was attached to the table, and then the outer frame of the magnet TMD was pulled to the left by an external force. The displacement of the magnet TMD was measured with the ruler, and the force measuring device displayed the repulsive force of the magnet TMD.

The displacement-repulsive force is shown in Figure 5. When the displacement was 0, since the mass is in the central position, the repulsive force was also 0; however, as the displacement increased, the relation between the repulsive force and the displacement became nonlinear. When the displacement reached 15 mm or more, the repulsive force increased sharply, so it can be known the nonlinear characteristic of TMD. This study used a TMD with a permanent magnet to utilize the advantages of a variable repulsive force. At the initial seconds of vibration excitation, the TMD can respond quickly by activating the small repulsive force; during intense vibration, the sharply increasing repulsive force can protect the mass block against the stroke energy. Otherwise, the mathematical result is to be identical to the experimental response, which suggests that the mathematical model of the permanent magnet can yield estimates of the tuned mass damper system.

**2.3. Mathematical Modeling.** A systemic model of a jackup offshore platform with a magnet TMD can be considered as a generalized structure, consisting of a main structure of the offshore platform and substructure of the magnet TMD. The general structure ( $m_1 + m_2$ ) includes the main structure of the offshore platform ( $m_1$ ) and the substructure of the TMD ( $m_2$ ), as shown in Figure 6 that is a simplified diagram of Figure 2(a).

The dynamic model can be expressed as

$$m_1 \ddot{x}_1 + c_1 \dot{x}_1 + k_1 x_1 - F_r = -m_1 \ddot{x}_V, \quad (5)$$

$$m_2 \ddot{x}_2 + F_r = -m_2 \ddot{x}_V, \quad (6)$$

where  $m_1$ ,  $c_1$ , and  $k_1$  are the mass, damping coefficient, and stiffness coefficient of the main structure, respectively;  $m_2$  is the mass of the substructure; and  $\ddot{x}_V$  is the acceleration vector of the seismic loads.  $x_1$  and  $x_2$  are the displacements of main structure and substructure, respectively.  $F_r$  is the repulsive force of the permanent magnets, as shown in (4).

As shown in Figure 7, numerical simulation and experimental investigations can constrain the displacements of the offshore platform with the magnet TMD, when it is subjected to seismic shaking represented as sinusoidal excitation. The frequency response comparison results between experiment and simulation is shown in Figure 8. The simulation response is observed to be identical to the experimental response over the entire time period, which suggests that the analytical method can yield estimates of the

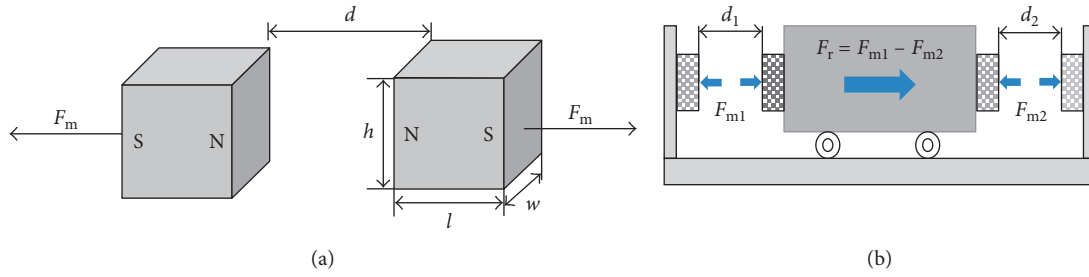


FIGURE 3: The calculation diagram of permanent magnet repulsive force. (a) The repulsive force of two permanent magnets; (b) the repulsive force of the magnet tuned mass damper.

TABLE 1: Material parameters of the magnet.

Length ( $l$ )	Width ( $w$ )	Height ( $h$ )	Magnetic property ( $B_r$ )	Permeability of space ( $\mu_0$ )
5 mm	15 mm	15 mm	0.337 T	$4\pi \times 10^{-7}$

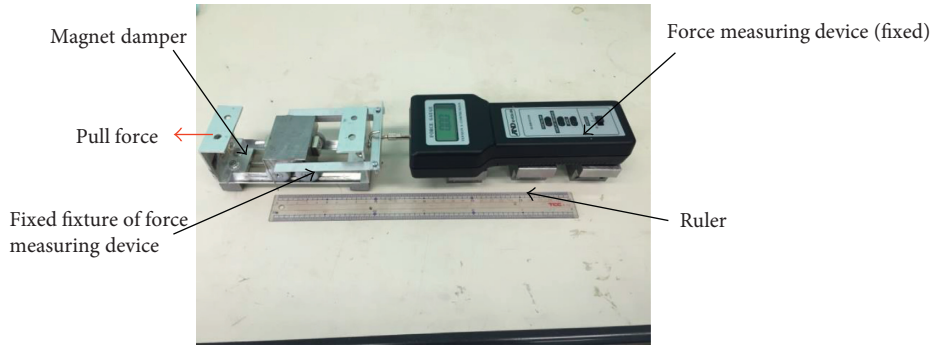


FIGURE 4: Force measurement setup.

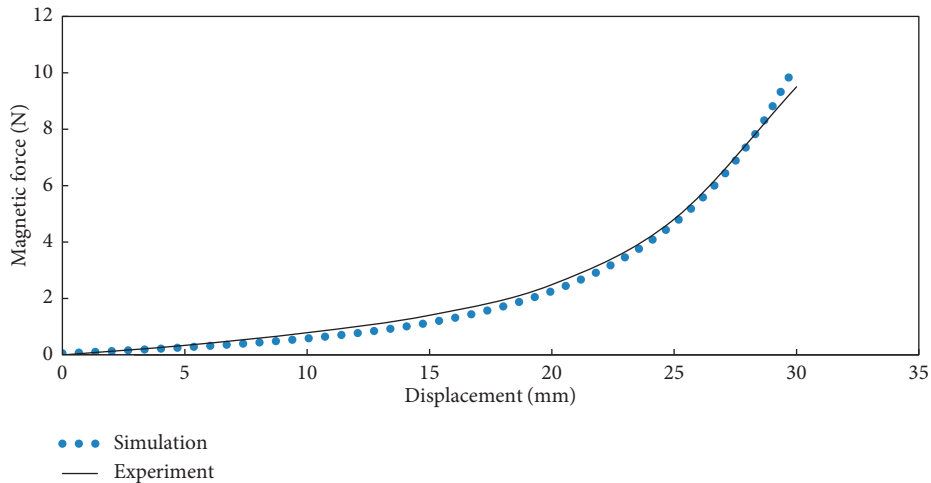


FIGURE 5: Repulsive force results by the simulating and experimental studies.

damper system response under sinusoidal signal excitations and sweep waves with good accuracy.

Before the experiment, to demonstrate the effectiveness of the proposed TMD, the results are presented on the

numerical studies in this section as shown in Figure 9. Three kinds of seismic waves were excited on the offshore platform model; it can be seen the proposed magnet TMD can effectively reduce the seismic damage of the system. For

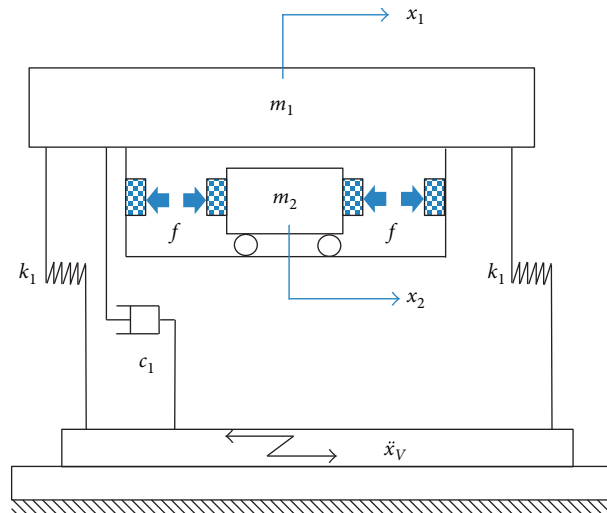


FIGURE 6: Systemic model of a jackup offshore platform with the magnet damper.

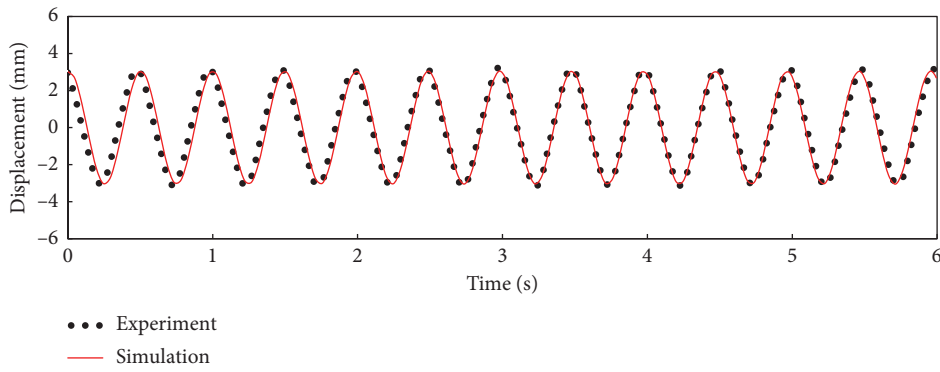


FIGURE 7: Displacements of the offshore platform under sinusoidal excitation.

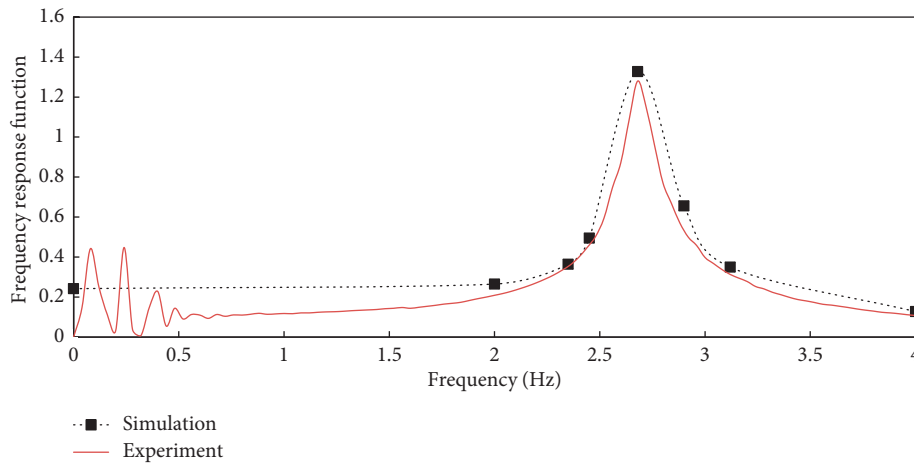


FIGURE 8: Frequency responses of the model offshore platform under sweep wave.

instance, the maximum peak value can be reduced about 30%; the vibration during the entire earthquake period can be reduced about 18% by the magnet TMD. In order to verify

the performance of the magnet TMD, the vibration experiment was performed for uncontrolled and controlled TMD system.

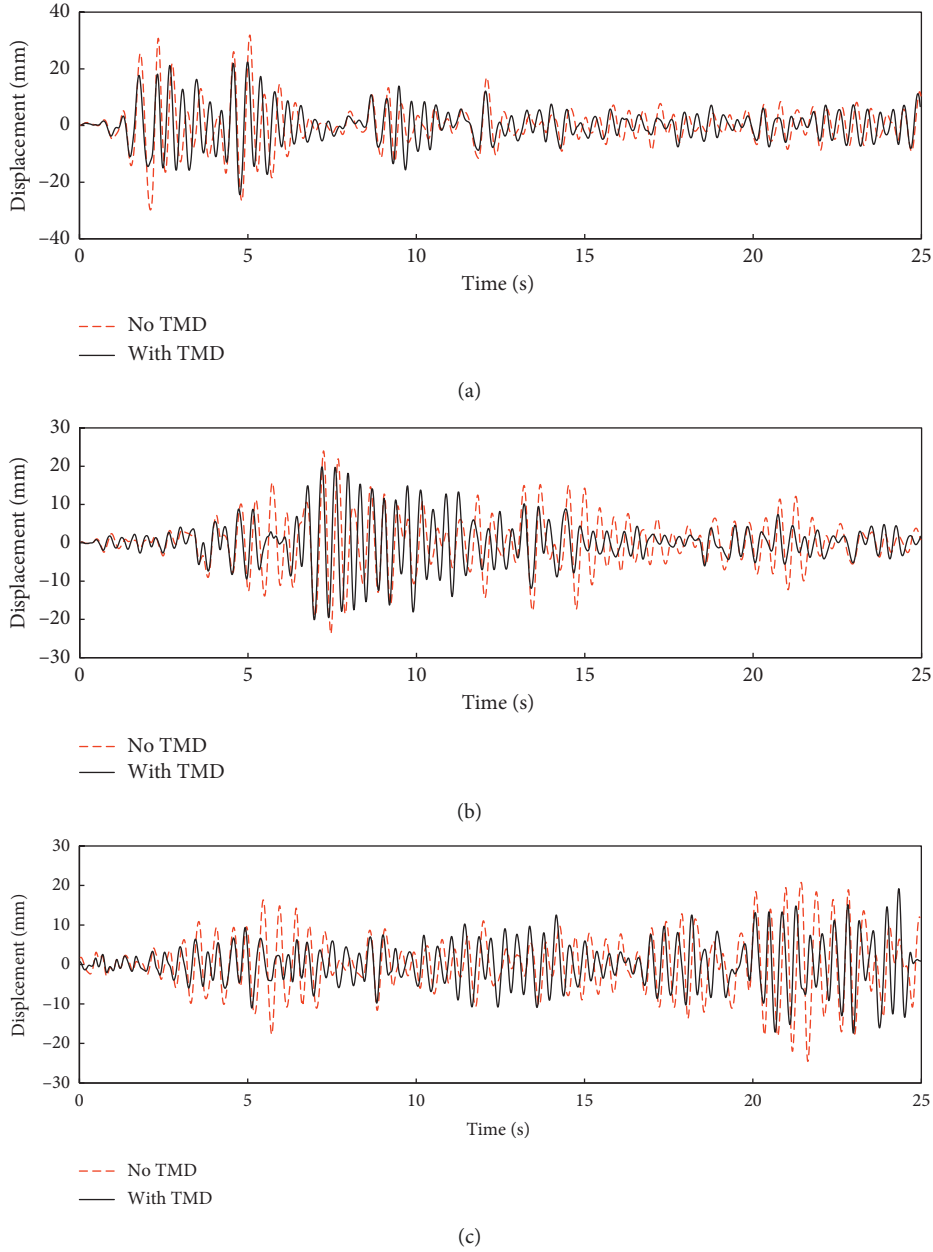


FIGURE 9: Displacement responses of the platform subjected to the three earthquake-induced seismic waves by simulation. (a) Displacement time series under the El-Centro NS seismic wave by simulation; (b) displacement time series under the Taft EW seismic wave by simulation; (c) displacement time series under the Fukushima NS seismic wave by simulation.

**2.4. Evaluation Index.** The root mean square (RMS) of the displacement or acceleration response can be expressed as

$$\text{RMS} = \sqrt{\frac{1}{n} \sum_{i=1}^n y_i^2}, \quad (7)$$

where  $y_i$  is the sampling value of the displacement or acceleration response.

To evaluate effectiveness of the vibration reduction during the entire earthquake period, an evaluation index was proposed as follows:

$$J = \frac{\text{RMS}_{\text{ctrl}}}{\text{RMS}_{\text{unctrl}}}, \quad (8)$$

where  $\text{RMS}_{\text{ctrl}}$  and  $\text{RMS}_{\text{unctrl}}$  are the RMS values of the displacement or acceleration responses of the main structure during the entire earthquake period, for the cases with and without the TMD system, respectively.

To evaluate the maximum response reduction, a maximum peak value was selected as  $y_{\max} = \max\{y_i\}$ . Then, a relative ratio of the maximum peak values can be obtained as

$$\beta = \frac{y_{\max\text{-unctrl}} - y_{\max\text{-ctrl}}}{y_{\max\text{-unctrl}}}, \quad (9)$$

where  $y_{\max\text{-ctrl}}$  and  $y_{\max\text{-unctrl}}$  are the maximum peak values of the displacement or acceleration response of the main structure, with and without the TMD system, respectively.

### 3. Experiment

**3.1. Setup.** As shown in Figure 10, the testing system comprised a personal computer, vibration signal generator, amplifier, shaker, offshore platform system, and fast Fourier transform analyzer. In the experiment, the sand height was 80 mm and the water depth was 400 mm. The mass of the offshore platform of the main structure ( $m_1$ ) was 2.346 kg, and the mass of the TMD ( $m_2$ ) was 0.591 kg. The damping coefficient was determined experimentally as 0.012. The offshore platform was placed in a water tank that was fixed to the shaker, which simulated the seismic motion.

Three types of earthquake-induced seismic waves (El-Centro NS, Taft EW, and Fukushima NS) were generated by the signal generator and fed to the shaker to evaluate the effectiveness of the vibration control system. The El-Centro NS was the NS component recorded at the Imperial Valley Irrigation District substation in El-Centro, California, USA on May 18, 1940. The earthquake had a magnitude of 6.9, and the peak acceleration was  $341 \text{ cm/s}^2$ . The Taft EW was the EW component recorded at Kern County, California, USA on July 21, 1952. The magnitude of the earthquake was 7.7, and the peak acceleration was  $175.9 \text{ cm/s}^2$ . Fukushima NS refers to the NS component recorded in Japan on March 11, 2011. The earthquake magnitude was 9.0 with a peak acceleration of  $341 \text{ cm/s}^2$ . The recording time for each of the three seismic waves was 25 s, and the sampling frequency was 50 Hz.

**3.2. Experimental Process.** Initially, the magnet TMD substructure was installed at the bottom of the model platform to measure the first natural frequency of the whole structure. The input signal was a 0–4 Hz sweep signal. The peak frequency response function for the platform was centred at 2.56 Hz, as shown in Figure 11(a).

The second step was to remove the magnet TMD from the platform and attach it to the shaker. Then, the spring stiffness of the magnet TMD was adjusted so that the first natural frequency of the magnet TMD was the same as that of the platform. The response of the magnet damper to the 0–4 Hz sweep sinusoid signal is shown in Figure 11(b) for four constant voltage levels, 2.8, 3, 3.2, and 4 V. Due to the nonlinear equivalent spring stiffness of the magnet damper, the obtained resonance curve of the magnet TMD has an unstable frequency character as shown in Figure 11(b). The nonlinear magnet TMD is unique in its ability to have a wide effective frequency bandwidth (1.5–3.5 Hz) which improves the performance of the passive vibration damper.

In the next step, three seismic waves were generated by the signal generator and fed to the shaker to evaluate the effectiveness of the vibration control system. The displacement and acceleration of the offshore platform and the

relative displacement between the offshore platform and the magnet TMD were recorded.

### 4. Results

**4.1. Amplitude Response Analysis.** Figures 12 and 13 show the time series of the responses for the main structure with and without the magnet TMD, under the excitations of the three kinds of seismic waves. The experimental results show a significant decrease in the peak values of the displacement and acceleration responses when the magnet TMD was attached to the main structure compared with those without the magnet TMD. This decreasing tendency was more significant for the acceleration responses. These results indicate that the control performance of the magnet TMD is as effective as an energy dissipation device for the reduction of the main structural response.

It is particularly important for vibration suppression under excitation by seismic waves that the magnet TMD can effectively reduce relatively high-amplitude displacements and accelerations. These high-amplitude displacements occurred during the early period of the test, and the magnet TMD responded quickly to these early vibration excitations. For the relatively low-amplitude displacements and accelerations, the effective reduction caused by the magnet TMD was small; however, these low-amplitude local effects contributed only a small portion of the overall platform vibration.

**4.2. Frequency Response Analysis.** The PSD curves under three kinds of seismic waves are presented in Figures 14 and 15, respectively. The high amplitude of the PSD is around 2.5 Hz~3 Hz for the case without TMD control, because the resonance reaction of the main structure occurred at around this frequency range. Therefore, when the TMD control was applied, it was very effective in reducing the vibration response of the main structure; in particular, the peak responses are reduced considerably around the 2.5 Hz~3 Hz frequency domain.

The overall vibration response can be decreased significantly by reducing the first-mode vibration; the PSD curves demonstrate the effective reduction in vibration of the structure when fitted with a magnet TMD. Therefore, a single damper tuned to the fundamental mode is adequate for reducing the structural vibration under earthquake excitations. Investigation of the frequency regions outside the fundamental frequency band revealed no negative effects in the nondominant frequency regions.

**4.3. Evaluation Index.** The control performance was evaluated by the application of the indices  $\beta$  and  $J$ , which are defined in (8) and (9), respectively. The  $J$  index is the ratio of the RMS values of the displacements or accelerations of the offshore platform, with and without the TMD control. The  $\beta$  index is the relative ratio of the peak values between the cases, with and without the TMD control.

As shown in Table 2, the  $J$  values for the displacement response are  $>0.79$ , which indicates that the vibration of the platform was significantly improved during the entire



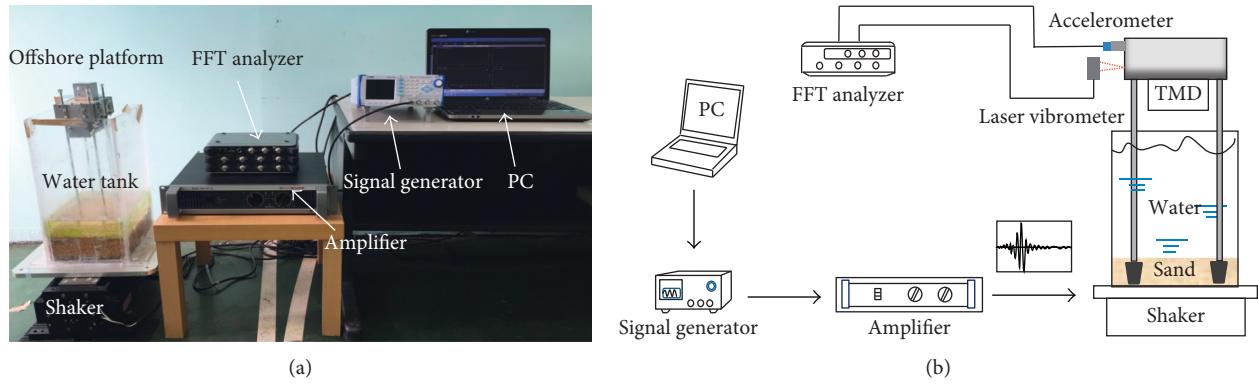


FIGURE 10: Diagram of the experimental system (PC: personal computer, TMD: tuned mass damper, and FFT Analyzer: fast Fourier transform analyzer). (a) Diagram of the experimental setting; (b) flowchart of the experiment system.

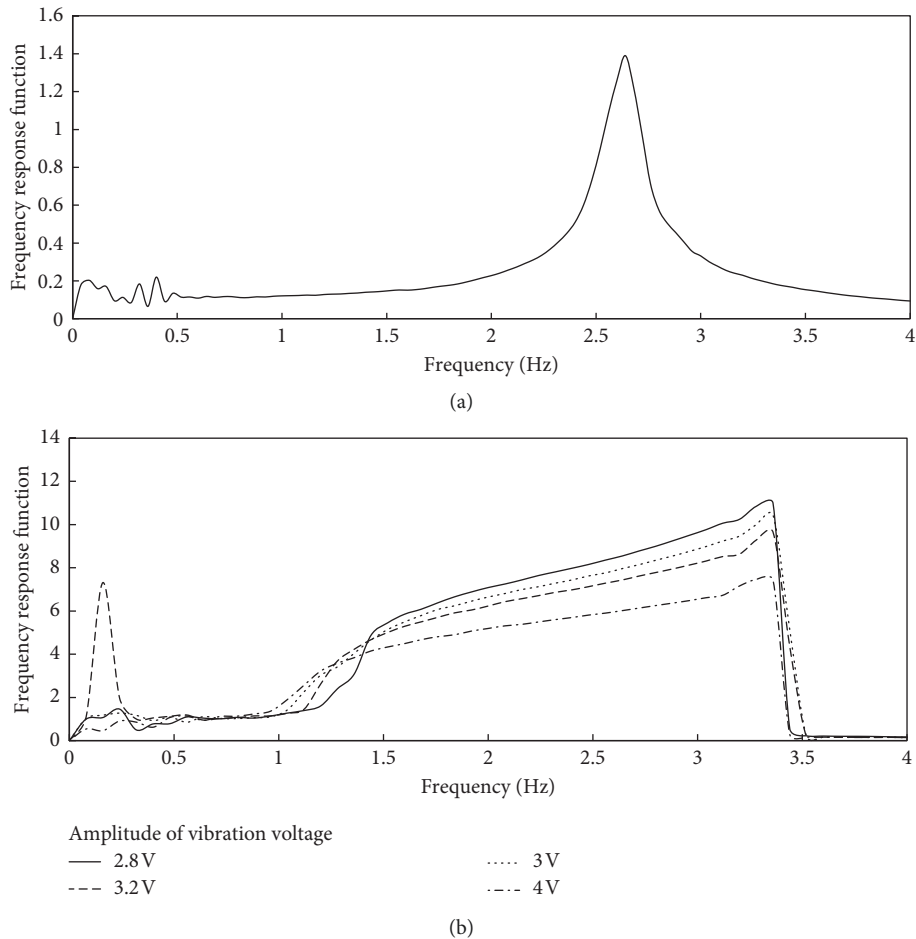


FIGURE 11: Frequency responses of the model offshore platform and magnet damper. Frequency response of the (a) model offshore platform and (b) magnet damper at different vibration amplitudes.

earthquake, period when the TMD was used. Moreover, by analysis of the  $\beta$  values, it shows that a reduction of  $>0.20$  was accomplished for the peak displacement response by the application of the TMD system.

For the acceleration displacement response, the  $J$  values are  $>0.78$ , which means the dynamic performance was also improved considerably throughout the entire excitation period. Similarly, the  $\beta$  values are  $>0.38$ , which means that

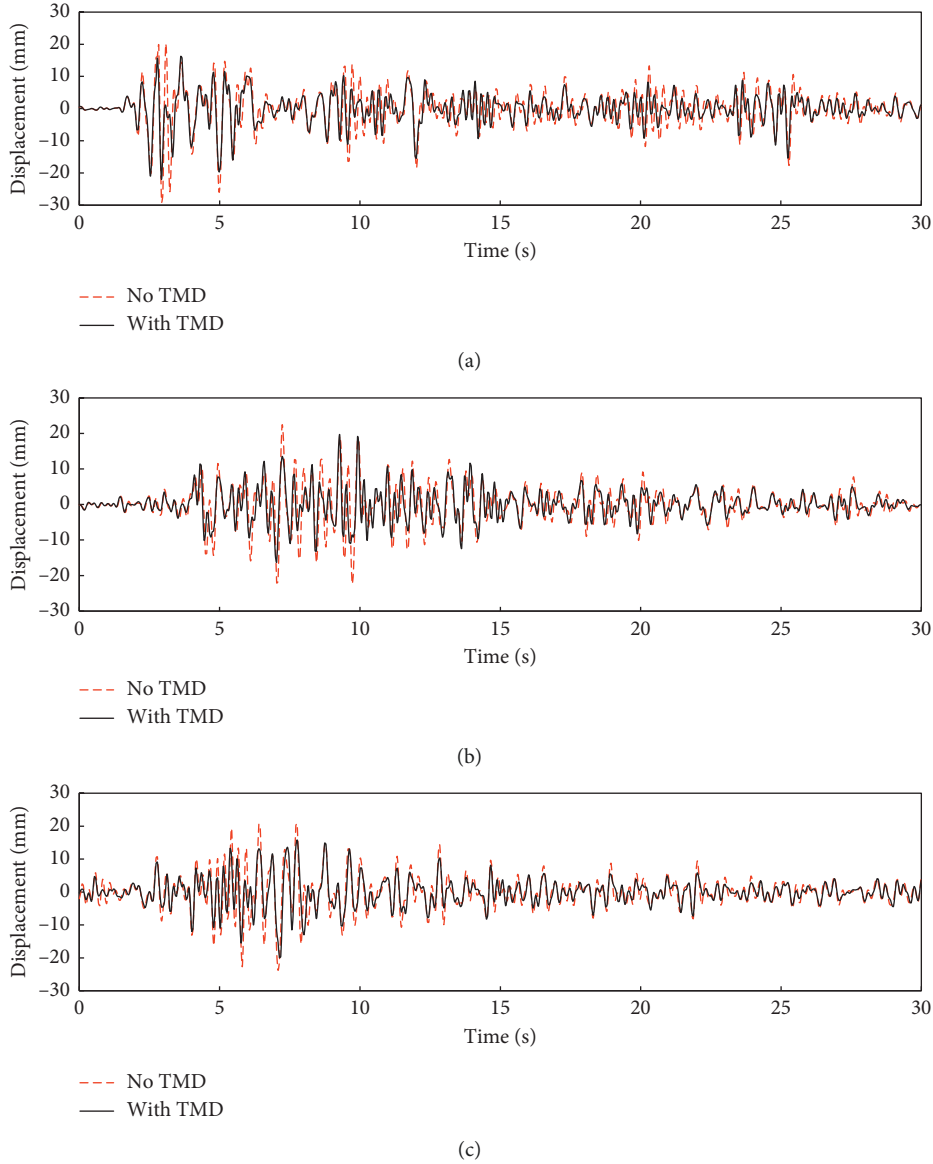


FIGURE 12: Displacement responses of the platform subjected to the three earthquake-induced seismic waves by experiment. Displacement time series under the (a) El-Centro NS seismic wave, (b) Taft EW seismic wave, and (c) Fukushima NS seismic wave.

the peak response was also decreased by the application of the TMD system.

## 5. Discussion

**5.1. High Response Characteristics.** The duration of an earthquake excitation is generally short, and the maximum influence on the platform's deformation occurs mainly during the initial seconds. Therefore, it is critical that the high response speed of the TMD occurs within the first few seconds of excitation. To achieve this goal, this study proposed a passive TMD without a damper to improve the high response performance under critical earthquake loads. For convenience, the nonlinear magnet repulsive force is seen as a nonlinear spring, so the system vibration equation can be expressed as

$$\begin{aligned} m_1 \ddot{x}_1 + c_1 \dot{x}_1 + k_1 x_1 - k_m (x_2 - x_1) &= -m_1 \ddot{x}_V, \\ m_2 \ddot{x}_2 + k_m (x_2 - x_1) &= -m_2 \ddot{x}_V, \end{aligned} \quad (10)$$

where  $k_m$  is the nonlinear stiffness coefficient of the substructure.

The central difference method [29] is used to numerically solve the above equations. A time-marching scheme for the forward difference method is used, where  $x^{(i)} = x(t = t_i)$  and the time interval is  $\Delta t = t_{i+1} - t_i$ . The differential acceleration and velocity can be expressed as

$$\begin{aligned} \ddot{x}^{(i)} &= \frac{x^{(i+1)} - 2x^{(i)} + x^{(i-1)})}{\Delta^2 t}, \\ \dot{x}^{(i)} &= \frac{x^{(i+1)} - x^{(i-1)})}{2\Delta t}. \end{aligned} \quad (11)$$

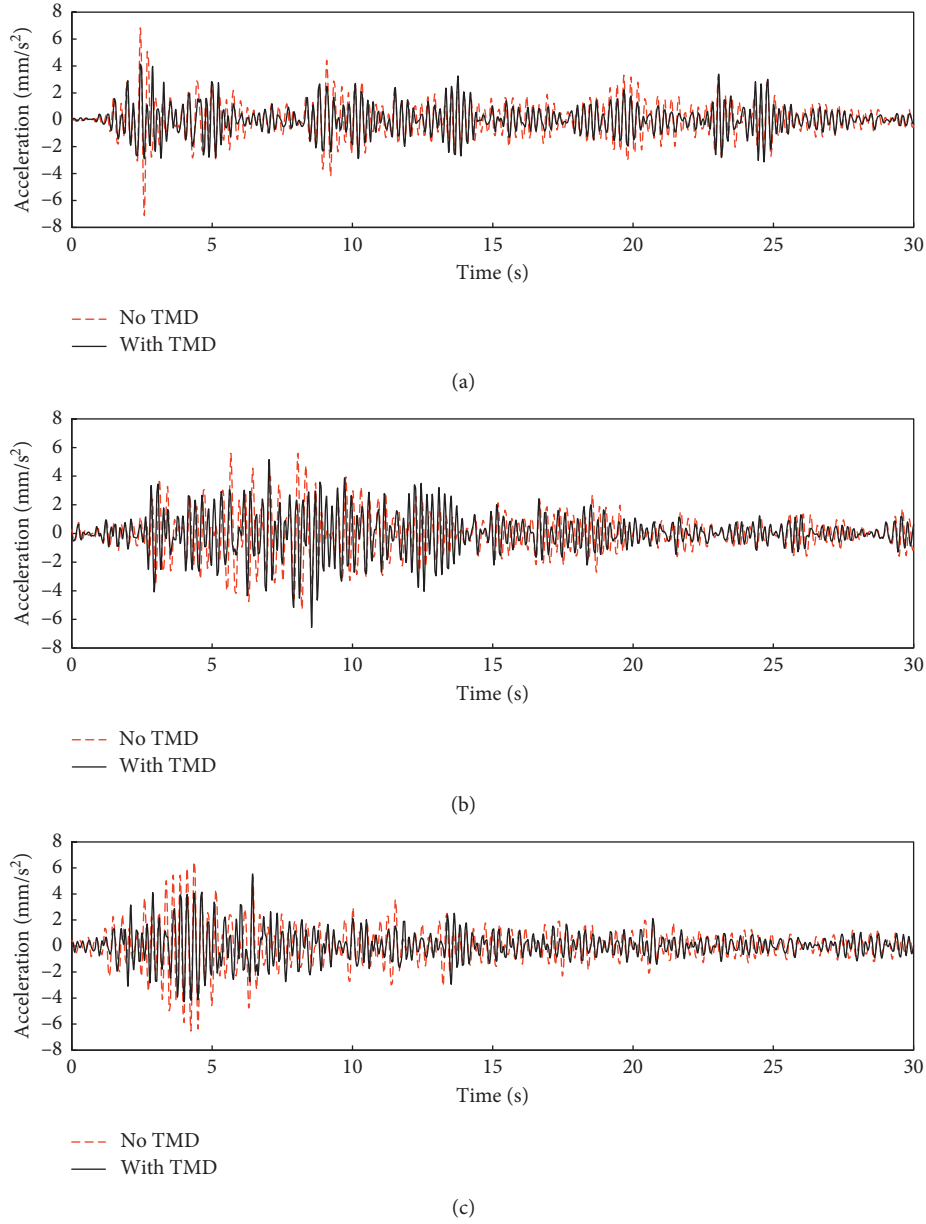


FIGURE 13: Acceleration responses of the platform subjected to the three earthquake-induced seismic waves by experiment. Acceleration time series under the (a) El-Centro NS seismic wave, (b) Taft EW seismic wave, and (c) Fukushima NS seismic wave.

Equations (6) and (7) can be substituted into (1) and (2) to calculate the displacement difference as

$$x_1^{(i+1)} = \frac{(2m_1 - k_1 \Delta^2 t - k_2 \Delta^2 t)x_1^{(i)} + k_m^{(i)} \Delta^2 t x_2^{(i)} + (-m_1 + 0.5c_1 \Delta t)x_1^{(i-1)} - m_1 \ddot{x}_v \Delta^2 t}{m_1 + 0.5c_1 \Delta t}, \quad (12)$$

$$x_2^{(i+1)} = \frac{(2m_2 - k_m^{(i)} \Delta^2 t)x_2^{(i)} + k_m^{(i)} \Delta^2 t x_1^{(i)} - m_2 x_2^{(i-1)} - m_2 \ddot{x}_v \Delta^2 t}{m_2}. \quad (13)$$

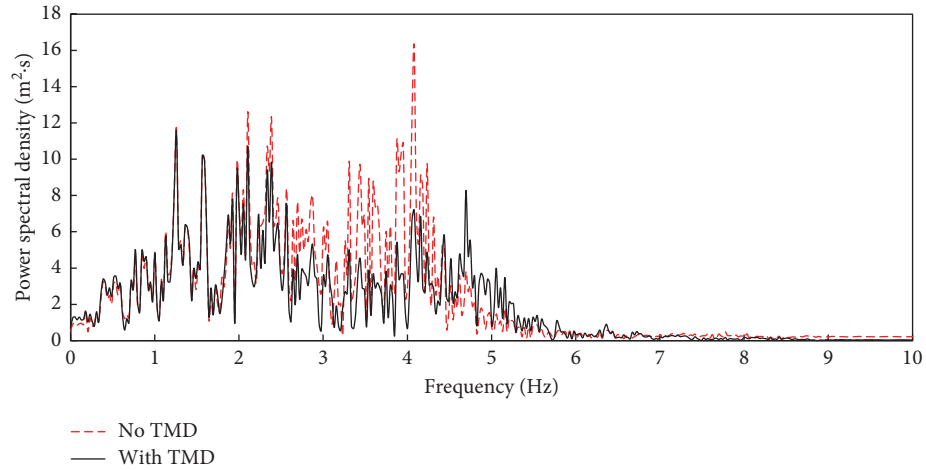
By applying the central difference method, the displacements of the substructure and the main structure during the

first 5 s of an excitation can be obtained. The initial conditions of the main structure can be expressed as

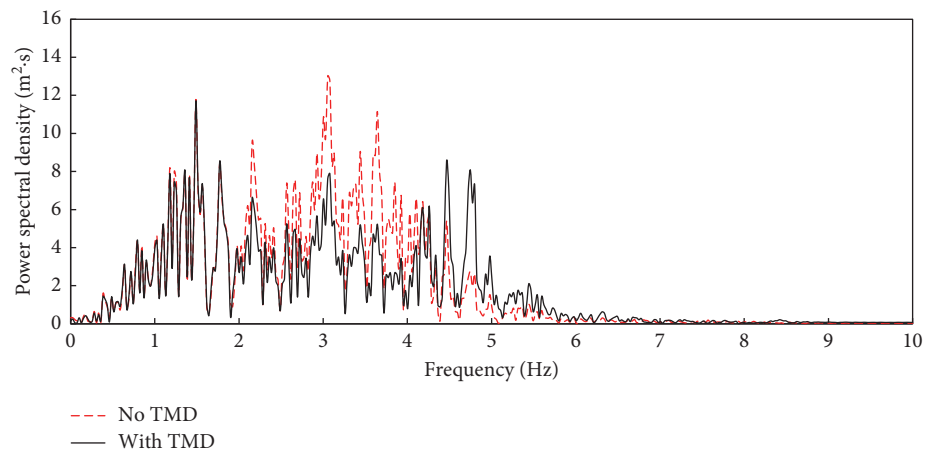
$$\begin{aligned} x_1^{(0)} &= 0, \\ x_2^{(0)} &= 0, \end{aligned} \quad (14)$$

$$\begin{aligned} \dot{x}_1^{(1)} &= 0, \\ \dot{x}_2^{(1)} &= 0. \end{aligned} \quad (15)$$

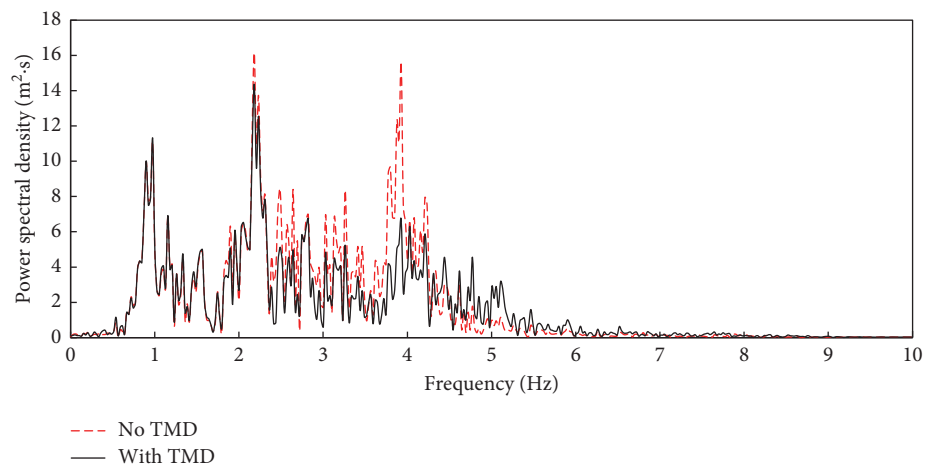
When the initial conditions of (14) and (15) are substituted into (12) and (13), the next-step differential displacements  $x_1^{(2)}$  and  $x_2^{(2)}$  can be obtained as follows:



(a)

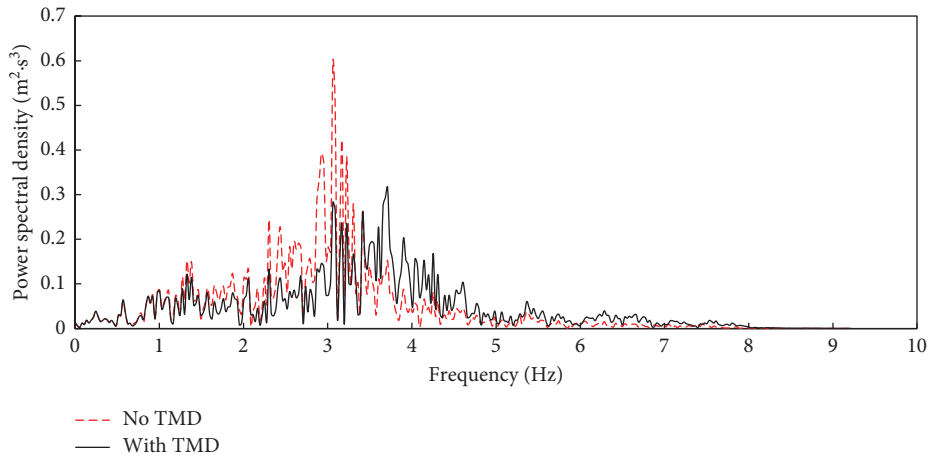


(b)

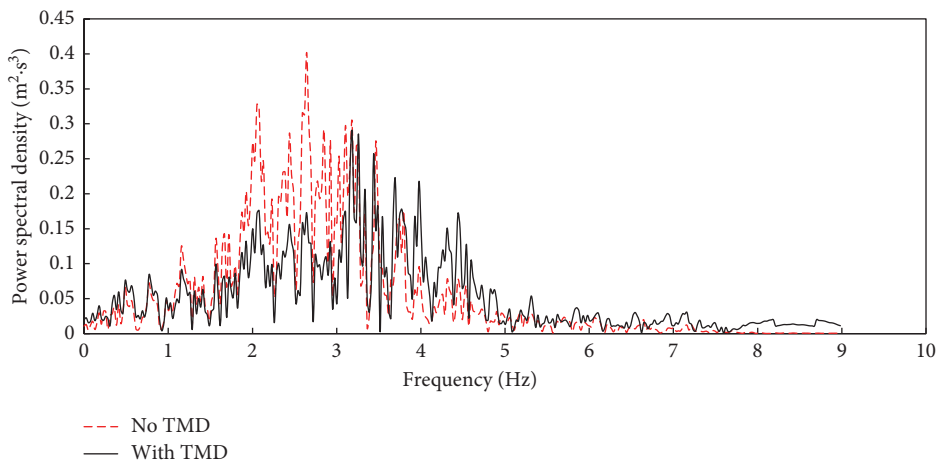


(c)

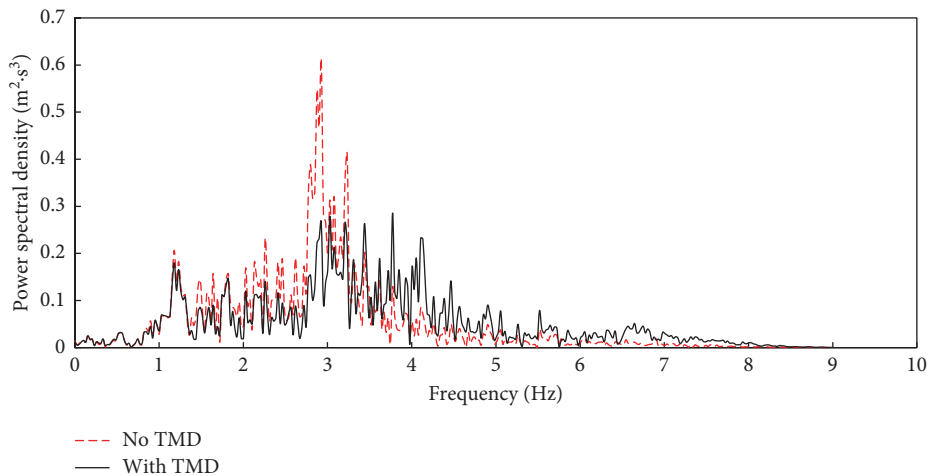
FIGURE 14: Power spectral density of the displacement under earthquake-induced seismic wave excitation. Power spectral density of the displacement for the (a) El-Centro NS earthquake seismic wave, (b) Taft EW earthquake seismic wave, and (c) Fukushima NS earthquake seismic wave.



(a)



(b)



(c)

FIGURE 15: Power spectral density of the acceleration under earthquake-induced seismic wave excitation. Power spectral density of the acceleration for the (a) El-Centro NS seismic wave, (b) Taft EW seismic wave, and (c) Fukushima NS seismic wave.

TABLE 2: Results of the evaluation indices.

Seismic excitation	Displacement response		Acceleration response	
	$\beta$	$J$	$\beta$	$J$
El-Centro NS	0.196	0.790	0.399	0.795
Taft EW	0.397	0.807	0.542	0.941
Fukushima NS	0.235	0.815	0.380	0.776

$$x_1^{(2)} = \frac{-m_1 \ddot{x}_V \Delta^2 t}{m_1 + 0.5c_1 \Delta t}, \quad (16)$$

$$x_2^{(2)} = -\ddot{x}_V \Delta^2 t.$$

The ratio of  $x_1^{(2)}$  and  $x_2^{(2)}$  can be expressed as

$$\frac{x_1^{(2)}}{x_2^{(2)}} = \frac{m_1}{m_1 + 0.5c_1 \Delta t} < 1. \quad (17)$$

It can be observed from (17), at the initial time that the displacement of the substructure  $x_2^{(2)}$  is always greater than the displacement of the main structure  $x_1^{(2)}$ , that is,  $x_2^{(2)} > x_1^{(2)}$ . Based on this theoretical analysis, an experiment was undertaken to investigate this high response phenomenon.

As illustrated in Figures 16(a) and 16(b), when the main structure begins to move under the earthquake excitation, the substructure also moves immediately. In addition, the displacement of the substructure is considerably greater than that of the main structure. This demonstrates that the substructure can achieve vibration suppression through its high response to the seismic excitations.

**5.2. Energy Absorption Characteristics.** To gain a more complete understanding of energy dissipation mechanisms and absorption characteristics of the magnet damping system, the energy dissipation is further examined under the two earthquake-induced seismic waves. This examination is of particular importance for seismic applications, in which the primary objective of TMD installation is to prevent damage to the structure of an offshore platform.

In Figures 17(a) and 17(b), the energy dissipation attained by the impact damping effect is presented for the El-Centro and Taft earthquake excitations. The energy reduction at the offshore platform is 17.6% with the El-Centro NS seismic wave and 18.4% under the Taft EW seismic wave. The simulation shows that impact damping plays a significant role in reducing the platform's vibration, which implies the usefulness of the magnet TMD even for offshore platforms exposed to large earthquake loads.

**5.3. Wide Frequency Range Characteristics.** Offshore platforms are mainly used for oil and gas extraction; during its working life, an offshore platform can experience uncertain conditions such as unknown system parameters and structure flexibility. These parameter perturbations and uncertainties mean that the natural frequency of the offshore platform may

change and may degrade the vibration control performance or even make the vibration control damper ineffective.

The main deficiency of the linear TMD is the detuning effect. The detuning effect occurs when the TMD's frequency is not tuned to the desired value, reducing the efficiency of the TMD damper. Unlike the linear TMD, the nonlinear magnet TMD has a wide efficient frequency domain, as shown in Figure 10.

We investigated the influence of a wideband magnet TMD system on the vibration reduction of the offshore platform model structure. In the experiment, we changed the mass of the offshore platform model structure which in turn changed the natural frequency of the offshore platform; the natural frequency of the offshore platform was set at 2.56 Hz, 2.68 Hz, 2.92 Hz, and 3.12 Hz, as shown in Figure 18(a). The magnet TMD can cover a frequency bandwidth with its medium tuned for the target frequency, as shown in Figure 18(b).

The evaluation parameters of the responses are shown for the main structure with and without the magnet TMD under the excitations of the El-Centro NS and Taft EW seismic waves (Figure 19). The magnet TMD system reduces the peak response vibration at different natural frequencies of the offshore platform. The peak response reduction of the acceleration responses is more than 17.2% in all the cases; for the displacement response, the peak response reduction is more than 16.9%. This demonstrates the high level of robustness and control efficiency of the magnet TMD system.

## 6. Conclusions

This study proposes a magnetic TMD system to mitigate damaging responses of an offshore platform exposed to significant earthquake-induced seismic waves. Moreover, a comprehensively numerical and experimental investigation was conducted to examine the vibration reduction performance and robust characteristics. By the experimental investigations, it is verified that the proposed magnetic TMD constitutes a simple but feasible measure, which can provide effective suppression within a wide frequency band and overcome response-delayed problems for vibration suppression under large earthquake loads. Furthermore, the main conclusions can be summarized as follows:

- (1) An experimental system was constructed based on a 1 : 200-scale model of an actual four-column jackup offshore platform, and then the experimental study was processed for the offshore platform both with and without the magnetic TMD system under the different seismic loads. The effectiveness of the magnetic TMD system were investigated by analyses of the amplitude and frequency responses, high response characteristics, energy absorption characteristics, and wide frequency range.
- (2) The experimental results indicated that the RMS ratios can reach to 79 % for displacement and 78 % for acceleration responses, and the vibrating excitations of the offshore platform were significantly

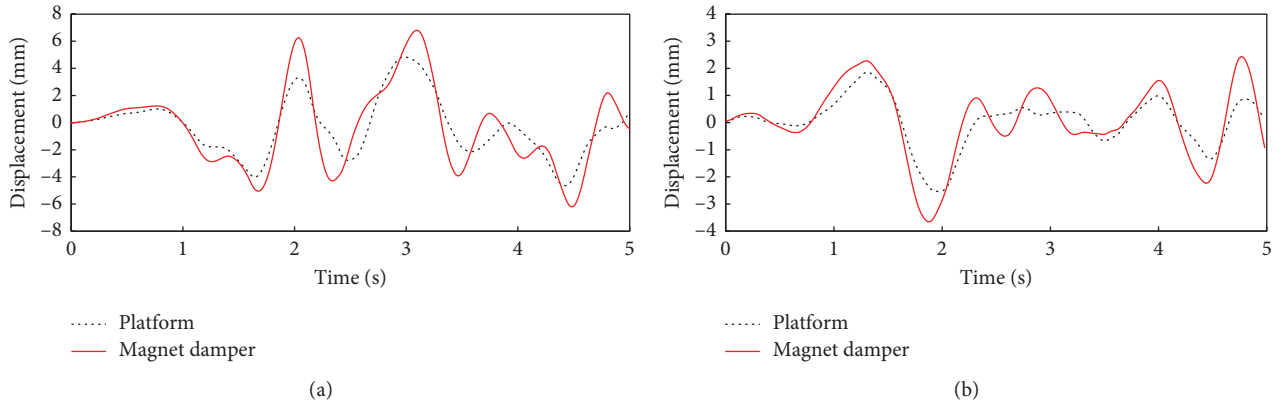


FIGURE 16: Displacement responses of platform and magnet damper under two seismic waves. Displacement responses for the (a) El-Centro NS seismic wave and (b) Taft EW seismic wave.

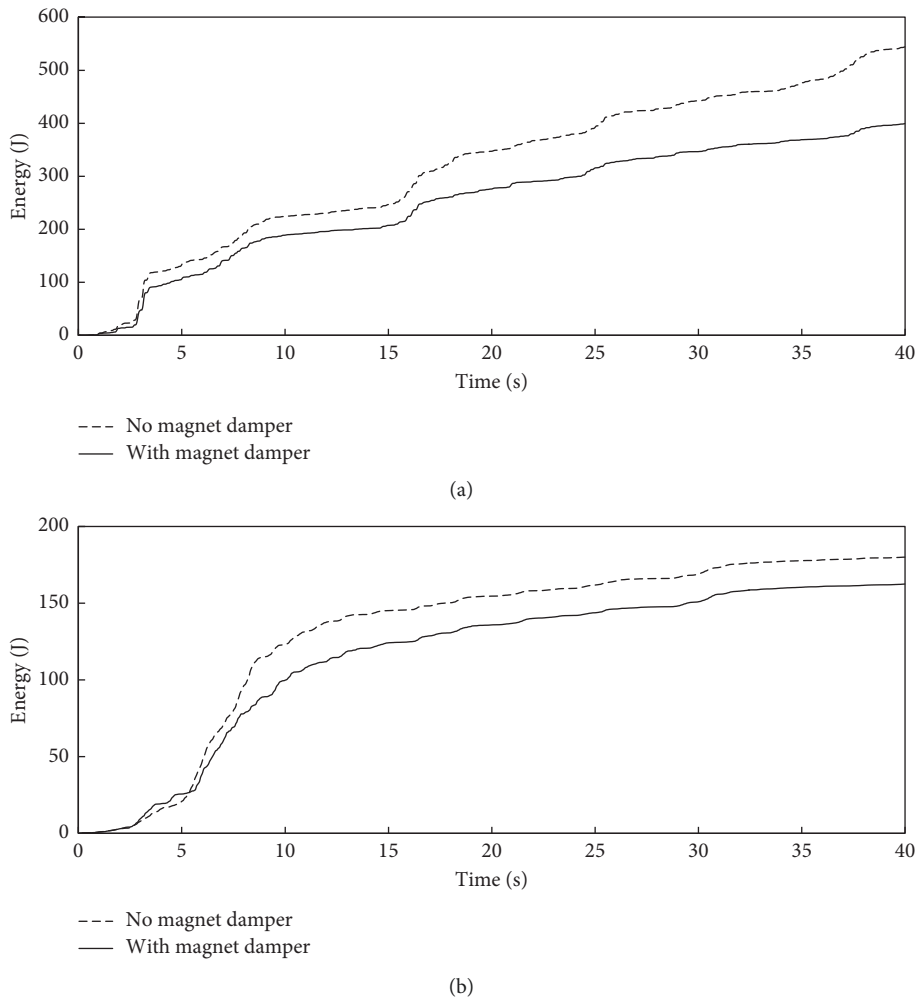


FIGURE 17: Cumulative energy dissipation for two seismic waves. Cumulative energy dissipation for the (a) El-Centro NS seismic wave excitation and (b) Taft EW seismic wave excitation.

improved for whole earthquake period. The relative ratio of the maximum peak values verified that more than 20% reduction was achieved for the

maximum peak of displacement response and more than 38% reduction for the acceleration response.

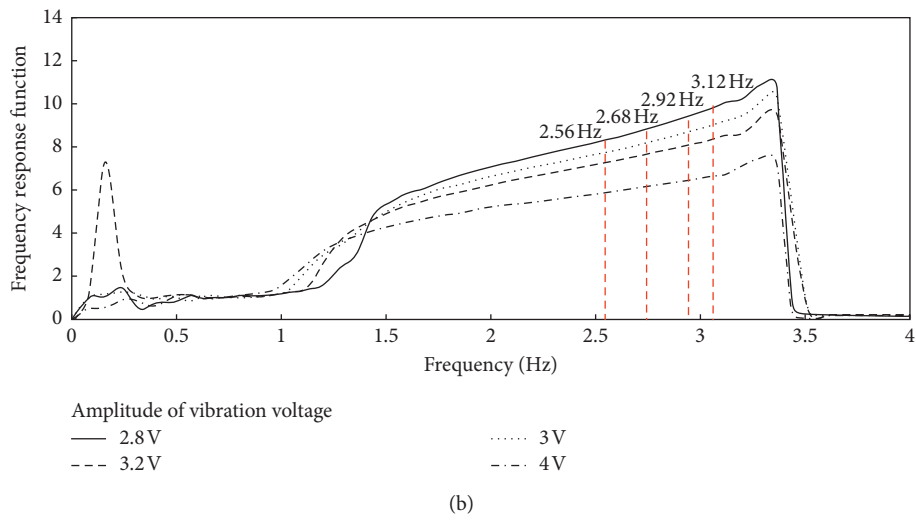
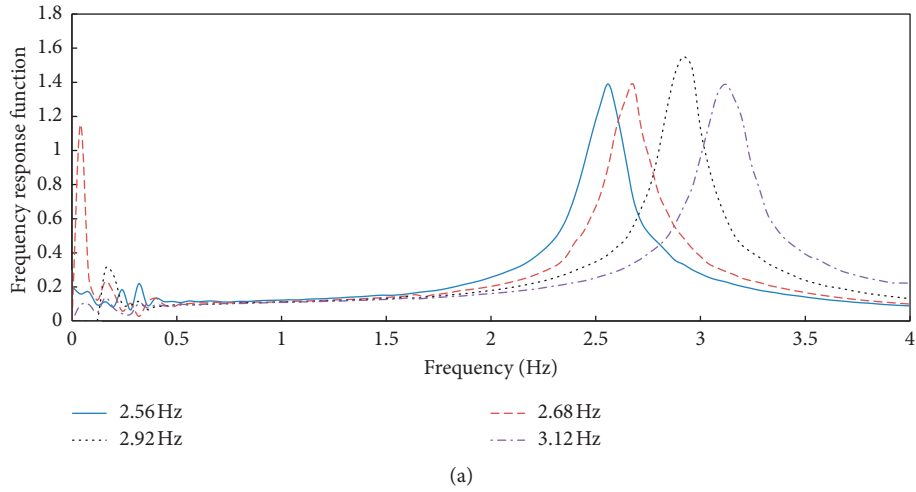


FIGURE 18: (a) Frequency response function of the offshore platform under different masses. (b) Natural frequency distributions of an offshore platform under the TMD's frequency response function.

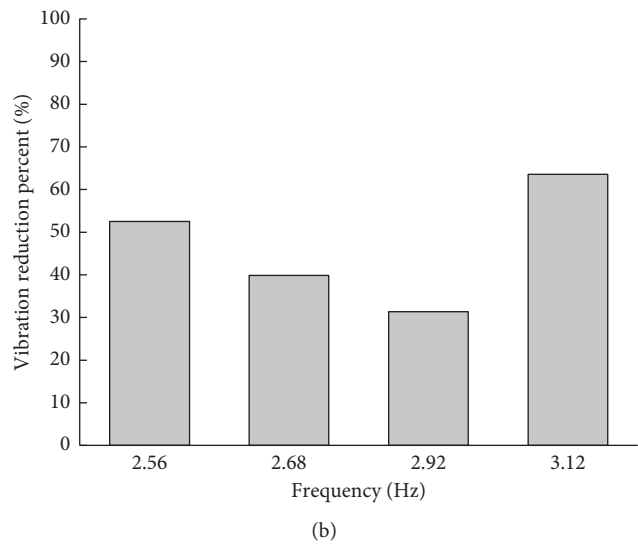
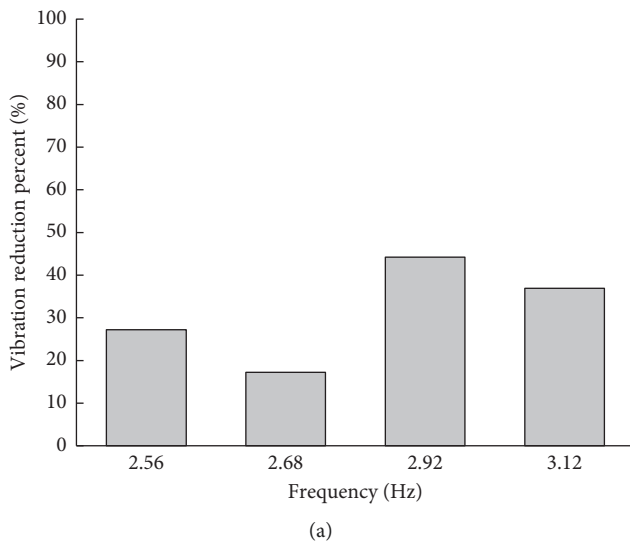


FIGURE 19: Continued.



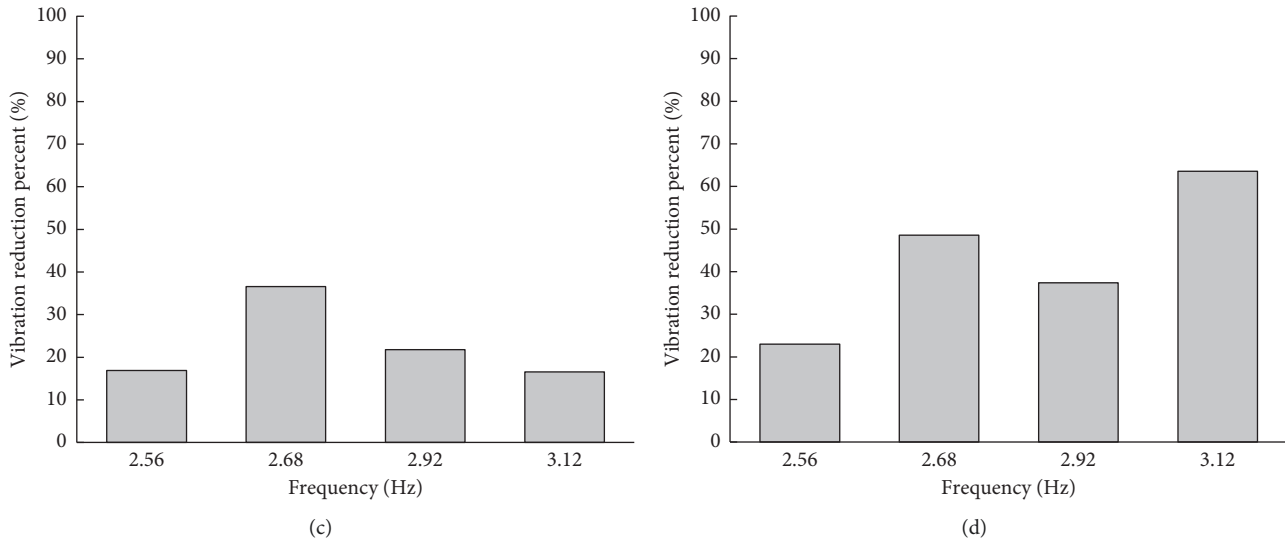


FIGURE 19: Experimental results for the evaluation parameters under two earthquake conditions. Evaluation indices of acceleration results under the (a) El-Centro NS seismic wave with various frequencies, (b) Taft EW seismic wave with various frequencies; evaluation indices of displacement results under the (c) El-Centro NS seismic wave with various frequencies. (d) Taft EW seismic wave with various frequencies.

- (3) In order to solve the time-delay problem at the first stage of the seismic load, this investigation indicates that the passively magnetic damper can move immediately during the first five seconds of earthquake excitation. Therefore, it reveals that the substructure can achieve vibration suppression through high-speed response to the seismic excitations in the initial seconds of the excitation.
- (4) In addition, the magnetic damper owned the wide frequency characteristic due to the nonlinear property. This nonlinear performance of the magnet damper increases the robustness of the system against changes in the working environment, thus enhancing its vibration reduction performance. On the contrary, when a critical earthquake happens, the distance of permanent magnets will get reduced and then the repulsive force will get increase rapidly. Furthermore, this nonlinear repulsive force of the magnetic TMD can protect the substructure colliding with the main structure, and it can reduce the damage of the offshore platform under the large vibration loads.

### Data Availability

The data that support the findings of this study are available from the first author by the email (wuqiong55@126.com), upon reasonable request.

### Conflicts of Interest

The authors declare that there are no conflicts of interest regarding the publication of this paper.

### Acknowledgments

The research was supported by the open fund for the Jiangsu Key Laboratory of Advanced Manufacturing Technology (no. HGAMTL-1707).

### References

- [1] X. Tang and L. Zuo, "Simulation and experiment validation of simultaneous vibration control and energy harvesting from buildings using tuned mass dampers," in *Proceedings of American Control Conference*, pp. 3134–3139, San Francisco, CA, USA, June 2011.
- [2] M. Ali and K. S. Moon, "Structural developments in tall buildings: current trends and future prospects," *Architectural Science Review*, vol. 50, no. 3, pp. 205–223, 2007.
- [3] T. A. Morgan and S. A. Mahin, "Development of a design methodology for seismic isolated buildings considering a range of performance objectives," in *Proceedings of 4th International Conference on Earthquake Engineering*, Taipei, Taiwan, October 2006.
- [4] K. M. Xu and T. Igusa, "Dynamic characteristics of multiple substructures with closely spaced frequencies," *Earthquake Engineering and Structural Dynamics*, vol. 21, no. 12, pp. 1059–1070, 1992.
- [5] H. Yamaguchi and N. Harnpornchai, "Fundamental characteristics of multiple tuned mass dampers for suppressing harmonically forced oscillations," *Earthquake Engineering and Structural Dynamics*, vol. 22, no. 1, pp. 51–62, 1993.
- [6] M. Abe and Y. Fujino, "Dynamic characteristics of multiple tuned mass dampers and some design formulas," *Earthquake Engineering and Structural Dynamics*, vol. 23, no. 8, pp. 813–835, 1994.

- [7] S. Wu, Y. Chen, and S. Wang, "Two-degree-of-freedom rotational-pendulum vibration absorbers," *Journal of Sound and Vibration*, vol. 330, no. 6, pp. 1052–1064, 2011.
- [8] H. Garrido, O. Curadelli, and D. Ambrosini, "Improvement of tuned mass damper by using rotational inertia through tuned viscous mass damper," *Engineering Structures*, vol. 56, pp. 2149–2153, 2013.
- [9] D. G. Kwag, J. S. Bae, and J. H. Hwang, "Experimental study for dynamic characteristics of an eddy current shock absorber," *Journal of the Korean Society for Aeronautical and Space Science*, vol. 35, no. 12, pp. 1089–1094, 2007.
- [10] C. Cai, W. Wu, and M. Araujo, "Cable vibration control with a TMD-MR damper system: experimental exploration," *Journal of Structural Engineering*, vol. 133, no. 5, pp. 629–637, 2007.
- [11] I. N. Ayala-Garcia, P. D. Mitcheson, E. M. Yeatman, D. Zhu, J. Tudor, and S. P. Beeby, "Magnetic tuning of a kinetic energy harvester using variable reluctance," *Sensors Actuators A: Physical*, vol. 189, no. 15, pp. 266–275, 2013.
- [12] R. P. Eason, C. Sun, A. J. Dick, and S. Nagarajaiah, "Attenuation of a linear oscillator using a nonlinear and a semi-active tuned mass damper in series," *Journal of Sound and Vibration*, vol. 332, no. 1, pp. 154–166, 2013.
- [13] L. D. Viet and N. B. Nghi, "On a nonlinear single-mass two-frequency pendulum tuned mass damper to reduce horizontal vibration," *Engineering Structures*, vol. 81, no. 15, pp. 175–180, 2014.
- [14] E. Gourdon, N. Alexander, C. Taylor, C. Lamarque, and S. Pernot, "Nonlinear energy pumping under transient forcing with strongly nonlinear coupling: theoretical and experimental results," *Journal of Sound and Vibration*, vol. 300, no. 3–5, pp. 522–551, 2007.
- [15] A. Vakakis, A. Kounadis, and I. Raftoyiannis, "Use of nonlinear localization for isolating structure from earthquake-induced motions," *Earthquake Engineering and Structural Dynamics*, vol. 28, no. 1, pp. 21–36, 1999.
- [16] A. Vakakis, L. Manevitch, O. Gendelman, and L. Bergman, "Dynamics of linear discrete systems connected to local, essentially nonlinear attachments," *Journal of Sound and Vibration*, vol. 264, no. 3, pp. 559–577, 2003.
- [17] T. H. Cheng and I. K. Oh, "A current-flowing electromagnetic shunt damper for multi-mode vibration control of cantilever beams," *Smart Materials and Structures*, vol. 18, no. 9, article 095036, 2009.
- [18] B. Farshi and A. Assadi, "Development of a chaotic nonlinear tuned mass damper for optimal vibration response," *Communications in Nonlinear Science and Numerical Simulation*, vol. 16, no. 11, pp. 4514–4523, 2011.
- [19] H. A. Sodano, J. S. Bae, D. J. Inman, and W. K. Belvin, "Concept and model of eddy current damper for vibration suppression of a beam," *Journal of Sound and Vibration*, vol. 288, no. 4–5, pp. 1177–1196, 2005.
- [20] H. A. Sodano, J. S. Bae, D. J. Inman, and W. K. Belvin, "Improved concept and model of eddy current damper," *Transaction of the ASME*, vol. 128, no. 3, pp. 294–302, 2006.
- [21] M. K. Kwak, M. I. Lee, and S. Heo, "Vibration suppression using eddy current damper," *Korean Society for Noise and Vibration Engineering*, vol. 13, no. 10, pp. 760–766, 2003.
- [22] J. S. Bae, M. K. Kwak, and D. J. Inman, "Vibration suppression of cantilever beam using eddy current damper," *Journal of Sound and Vibration*, vol. 284, no. 3–5, pp. 805–824, 2005.
- [23] C. Zhang and J. Ou, "Control structure interaction of electromagnetic mass damper system for structural vibration control," *Journal of Engineering Mechanics*, vol. 134, no. 5, pp. 428–437, 2008.
- [24] Y. B. Kim, W. G. Hwang, C. D. Kee, and H. B. Yi, "Active vibration control of a suspension system using an electromagnetic damper," *Proceedings of the Institution of Mechanical Engineers, Part D: Journal of Automobile Engineering*, vol. 215, no. 8, pp. 865–873, 2001.
- [25] R. Palomera-Arias, J. J. Connor, and J. A. Ochsendorf, "Feasibility study of passive electromagnetic damping systems," *Journal of Structural Engineering*, vol. 134, no. 1, pp. 164–170, 2008.
- [26] Q. Wu, X. Zhao, R. Zheng, and K. Minagawa, "High response performance of a tuned-mass damper for vibration suppression of offshore platform under earthquake loads," *Shock and Vibration*, vol. 2016, Article ID 7383679, 11 pages, 2016.
- [27] Q. Wu, X. Zhao, S. He, W. Tang, and R. Zheng, "A bufferable tuned-mass damper of an offshore platform against stroke and response delay problems under earthquake loads," *Shock and Vibration*, vol. 2016, Article ID 9702152, 12 pages, 2016.
- [28] Z. S. Chen and Y. M. Yang, "Stochastic resonance mechanism for wideband and low frequency vibration energy harvesting based on piezoelectric cantilever beams," *Acta Physics Science*, vol. 60, no. 7, 2011.
- [29] S. S. Rao, *Mechanical Vibrations*, Prentice Hall, Upper Saddle River, NJ, USA, 2010.



**Hindawi**

Submit your manuscripts at  
[www.hindawi.com](http://www.hindawi.com)

